

reprintAPS/123-QED

Thermodynamic geometry of black holes in $f(R)$ gravity

Saheb Soroushfar, Reza Saffari,^{*} and Negin Kamvar

Department of Physics, University of Guilan, 41335-1914, Rasht, Iran.

(Dated: May 4, 2016)

Abstract

In this paper, we consider three types (static, static charged and rotating charged) of black holes in $f(R)$ gravity. We study the thermodynamical behavior, stability conditions and phase transition of these black holes. It will be shown that, the number and type of phase transition points are related to different parameters, which shows the dependency of stability conditions to these parameters. Also, we extended our study to different thermodynamic geometry methods (Ruppeiner, Weinhold and GTD). Next, we investigate the compatibility of curvature scalar of geothermodynamic methods with phase transition points of the above black holes. In addition, we point out the effect of different values of spacetime parameters on stability conditions of mentioned black holes.

^{*}Electronic address: rsk@guilan.ac.ir

1. INTRODUCTION

The black hole is one of the most fascinating anticipations of Einstein's theory of General Relativity, which has been an adsorbent subject in theoretical physics for many years, and it has unknown issues yet. One of the most interesting aspects of studying black holes, is thermodynamics. The studies on black holes as a thermodynamic system is started with famous work of Hawking and Bekenstein [1–3], which is followed by other pioneering research of Padmanabhan [4],[5]. According to the black hole thermodynamics, the thermodynamic quantities of a black hole such as entropy and temperature are related to it's geometrical quantities such as horizon area and surface gravity [2], [6]. In recent years, the researches on the thermodynamic properties of the black holes have got a lot of interesting aspects. One of these aspects is stability of black holes. Heat capacity of a black hole must be positive in order to be in thermal stability [7]. Studying the heat capacity of a black hole provides a mechanism to study the phase transitions of the black holes. There are two types of phase transition; in the first one, the changes in the sign of the heat capacity denoted as a type of phase transition, in the other words, roots of the heat capacity represent phase transition points, so we call these phase transition type one. Another kind of phase transition obtains from divergencies of the heat capacity. This kind of phase transition is called the phase transition type two [7]. Some works on the normal thermodynamics of black holes shows that in many cases, one can not identify the detailed reasons irregularities of mass, temperature and heat capacity shown by the system. During the last few decades, many efforts have been made to introduce different concepts of geometry in to ordinary thermodynamics. Hermann [8] defined the implication of thermodynamic phase space as a differential manifold with a natural contact structure, in which there exist a special subspace of thermodynamic equilibrium states. Weinhold introduced an other geometric method in 1975 [9], in which a metric is defined in the space of equilibrium states of thermodynamic systems. Weinhold used the notion of conformal mapping from the Riemannian space to thermodynamic space. Weinhold's metric is defined as the Hessian in the mass representation as follows

$$g_{ij}^W = \partial_i \partial_j M(S, N^r), \quad (1)$$

where M is the mass, S is the entropy and N^r is the other extensive variables of the system. After that in 1979, Ruppeiner [10] defined a new metric which is the minus signed Hessian

in entropy representation and is given by

$$g_{ij}^R = -\partial_i \partial_j S(M, N^r). \quad (2)$$

The Ruppeiner's metric is conformally related to Weinhold's metric as follows [11], [12]

$$ds_R^2 = \frac{1}{T} ds_W^2, \quad (3)$$

where T is the temperature of the thermodynamic system.

Geometrothermodynamics (GTD) is the latest attempt in this way [13], [14]. Quevedo [13] introduced a general form of the legender invariant metric. The general form of the metric in *GTD* method is as follows

$$g = (E^c \frac{\partial \Phi}{\partial E^c}) (\eta_{ab} \delta^{bc} \frac{\partial^2 \Phi}{\partial E^c \partial E^d} dE^a dE^d), \quad (4)$$

in which

$$\frac{\partial \Phi}{\partial E^c} = \delta_{cb} I^b, \quad (5)$$

where E^a and I^b are the extensive and intensive thermodynamic variables and Φ is the thermodynamic potential.

There were some alternative and extended theories on General Relativity from the beginning it [15–17]. Some of new versions of these theories are trying to justify some observed anomalies in galactic scales (dark matter) and cosmological scales (dark energy) which leads to reinforce them, such as, scalar-tensor theories, brane world cosmology, Lovelock gravity and $f(R)$ gravity. Many different aspects, such as, cosmic inflation, cosmic acceleration, dark matter, correction of the solar system abnormalities, and also geodesic motion of test particle, have been studied in $f(R)$ gravity [17–27].

The main purpose of this paper, is to investigate that the thermodynamic geometric methods can be used to explain thermodynamics of black holes in $f(R)$ gravity, and it is organized as follows, in Sec. 2, we review a static black hole in $f(R)$ gravity, then we study the thermodynamic behavior and thermodynamic geometry methods for this black hole, In Sec. 3, also, we review a static charged black hole in $f(R)$ gravity and study the thermodynamic behavior and thermodynamic geometry methods for it, In Sec. 4, we review a rotating charged black hole in $f(R)$ gravity, then we investigate the thermodynamic behavior and thermodynamic geometry methods for it, as well, and final results are conclude in Sec. 5

2. STATIC BLACK HOLE IN $f(R)$ GRAVITY

In this section, we study the field equations for a static black hole in $f(R)$ gravity. The action depending on the Ricci scalar in a generic form is:

$$S = \frac{1}{2k} \int d^4x \sqrt{-g} f(R) + S_m. \quad (6)$$

Varying the action with respect to the metric results in the field equations as:

$$F(R)R_{\mu\nu} - \frac{1}{2}f(R)g_{\mu\nu} - (\nabla_\mu \nabla_\nu - g_{\mu\nu} \square)F(R) = kT_{\mu\nu}, \quad (7)$$

where $F(R) = \frac{df(R)}{dR}$ and $\square = \nabla_\alpha \nabla^\alpha$.

A generic form of the metric of the spherically symmetric spacetime we are considering is

$$ds^2 = -B(r)dt^2 + A(r)dr^2 + r^2(d\theta^2 + \sin^2\theta d\varphi^2), \quad (8)$$

where $A(r) = B(r)^{-1}$. The model employed for $f(R)$ gravity is given by

$$f(R) = R + \Lambda + \frac{R + \Lambda}{R/R_0 + 2/\alpha} \ln \frac{R + \Lambda}{R_c}, \quad (9)$$

In which, R_c is a constant of integration and $R_0 = 6\alpha^2/d^2$, where α , and d , are free parameters of the action, and also Λ is the cosmological constant. The metric solution up to the first order in the free parameters of the action is obtained as $B(r) = 1 - \frac{2m}{r} + \beta r - \frac{1}{3}\Lambda r^2$, where, $\beta = \alpha/d \geq 0$, is a real constant [26], [27].

2.1. Thermodynamic

In this section, we study the thermodynamic properties of this black hole. we could find the mass of the black hole M , in terms of its entropy S , and the radius of curvature of de Sitter space l , where l , is related to the cosmological constant Λ , through the relation [28]

$$\Lambda = \frac{3}{l^2}. \quad (10)$$

Using the relation between entropy S , and event horizon radius r_+ , ($S = \pi r_+^2$), we can write the mass as below,

$$M(S, l, \beta) = \frac{l^2 \pi^{\frac{1}{2}} \beta S + l^2 \pi S^{\frac{1}{2}} - S^{\frac{3}{2}}}{2l^2 \pi^{\frac{3}{2}}}. \quad (11)$$

The other thermodynamic parameters can be calculated by using the above expression as Temperature ($T = \frac{\partial M}{\partial S}$) and, heat capacity ($C = T \frac{\partial S}{\partial T}$) as a function of S , l and β ,

$$T = \frac{2\beta l^2 \pi^{\frac{1}{2}} S^{\frac{1}{2}} - 3S + l^2 \pi}{4l^2 \pi^{\frac{3}{2}} S^{\frac{1}{2}}}, \quad (12)$$

$$C = -\frac{4\beta l^2 \pi^{\frac{1}{2}} S^{\frac{3}{2}} - 6S^2 + 2l^2 \pi S}{l^2 \pi + 3S}. \quad (13)$$

We have obtained three thermodynamic parameters of this black hole and plotted all of them in terms of horizon radius r_+ , (see Figs. 1–3).

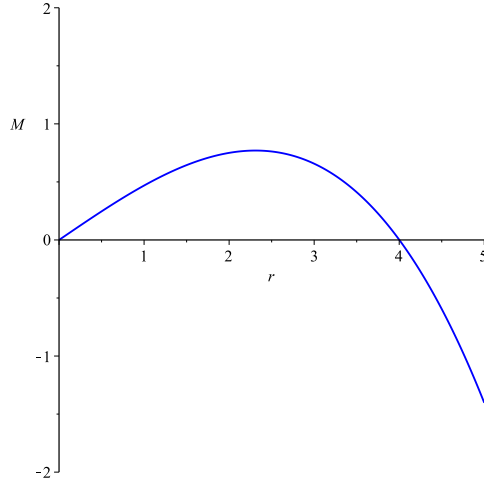


FIG. 1: Mass variation of a static black hole in terms of horizon radius r_+ for $l = 4.0$, $\beta = 10^{-4}$.

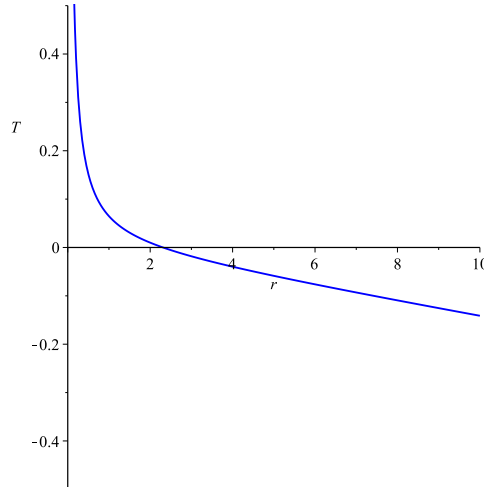


FIG. 2: Temperature variation of a static black hole in terms of horizon radius r_+ for $l = 4.0$, $\beta = 10^{-4}$.

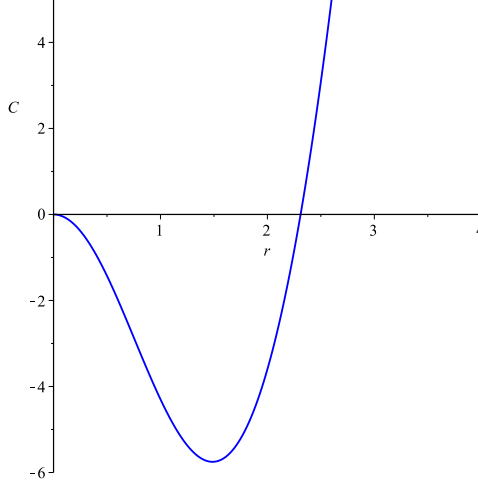


FIG. 3: Heat capacity variation of a static black hole in terms of horizon radius r_+ for $l = 4.0$, $\beta = 10^{-4}$.

In Fig.1, it can be seen that, mass of the black hole become zero at two points, $r_+ = r_{01}$ and $r_+ = r_{02}$ (we show the zero points of mass with r_{01} and r_{02}), in which, $r_{01} = 0$ and $r_{02} = 4.0$, and it reaches into a maximum value at $r_+ = r_m$ (we show the place of maximum value of mass with r_m), which is equal to 2.31. Also, it can be observed from Fig. 2, that, Temperature is positive only in a particular range of r_+ , then it reaches in to zero at, $r_+ = r_m$, and after that, it falls in to negative region, in which, it has nonphysical meaning. Finally, by plotting heat capacity of the black hole in terms of horizon radius, r_+ , in Fig. 3, we have shown that, this black hole has phase transition type one, in other words, in the range of, $0 < r_+ < r_m$, the heat capacity is in the negative region (unstable phase), then at, $r_+ = r_m$, it takes phase transition type one ($C(r_+ = r_m) = 0$), after that for, $r_+ > r_m$, it will be positive (stable).

2.2. Thermodynamic Geometry

Now, we construct the geometric structure for this black hole by applying the geometric technique of Weinhold, Ruppiner and GTD metrics of the system. In this case, the extensive variables are, $N^r = (l, \beta)$. According to Eq. (1), we can write the Weinhold metric for this system as below

$$g_{ij}^W = \partial_i \partial_j M(S, l, \beta), \quad (14)$$

$$\begin{aligned}
ds_W^2 &= M_{SS}dS^2 + M_{ll}dl^2 + M_{\beta\beta}d\beta^2 \\
&+ 2M_{Sl}dSdl + 2M_{S\beta}dSd\beta + 2M_{l\beta}dld\beta,
\end{aligned} \tag{15}$$

therefore

$$g^W = \begin{bmatrix} M_{SS} & M_{Sl} & M_{S\beta} \\ M_{lS} & M_{ll} & 0 \\ M_{\beta S} & 0 & 0 \end{bmatrix}. \tag{16}$$

The components of above matrix can be found using the expression of M , given in Eq. (11). We could calculate the curvature scalar of the Weinhold metric as,

$$R^W = 0, \tag{17}$$

so the Weinhold structure is flat for this black hole and, we can not explain phase transition of this thermodynamic system. Now, we use Ruppiner method, which is conformally transformed to Weinhold metric. Ruppiner metric is given by

$$ds_R^2 = \frac{1}{T} ds_W^2. \tag{18}$$

The correspond matrix with the metric components of Ruppiner method, is as follow,

$$g^R = \left(\frac{1}{T}\right) \begin{bmatrix} M_{SS} & M_{Sl} & M_{S\beta} \\ M_{lS} & M_{ll} & 0 \\ M_{\beta S} & 0 & 0 \end{bmatrix}, \tag{19}$$

which is equal to

$$g^R = \left(\frac{4l^2\pi^{\frac{3}{2}}S^{\frac{1}{2}}}{2l^2\pi^{\frac{1}{2}}S^{\frac{1}{2}}\beta - 3S + l^2\pi}\right) \begin{bmatrix} M_{SS} & M_{Sl} & M_{S\beta} \\ M_{lS} & M_{ll} & 0 \\ M_{\beta S} & 0 & 0 \end{bmatrix}. \tag{20}$$

The curvature of the Ruppiner metric is obtained as below,

$$R^R = \frac{4S^{\frac{5}{2}}l^2\pi^{\frac{1}{2}}\beta - 13S^{\frac{5}{2}}\pi^{\frac{1}{2}}l^2\beta - 3S^{\frac{5}{2}}\pi^{\frac{1}{2}}l^2\beta - 11S^2l^2\pi + 3S^3}{4S^3(2S^{\frac{1}{2}}\pi^{\frac{1}{2}}l^2\beta - 3S + l^2\pi)}, \tag{21}$$

which is singular at $S = 0$ and, $S = \frac{1}{3}l^2\pi(2\beta l(\frac{1}{3}l\beta + \frac{1}{3}\sqrt{l^2\beta^2 + 3}) + 1)$, for each solution of S , there exists a pair of r_+ , ($r_+ = \pm\sqrt{\frac{S}{\pi}}$), which can explain zero points in

this thermodynamic system. We avoid the negative values of this solution because it gives imaginary and negative roots. The values of these zero points are, $r_+ = 0$, and, $r_+ = r_m$. It is completely coincide with zero point of the temperature and the heat capacity (the phase transition point) of this black hole. The curvature scalar of Ruppeiner metric for this black hole with respect to horizon radius, r_+ , is demonstrated in Fig. 4.

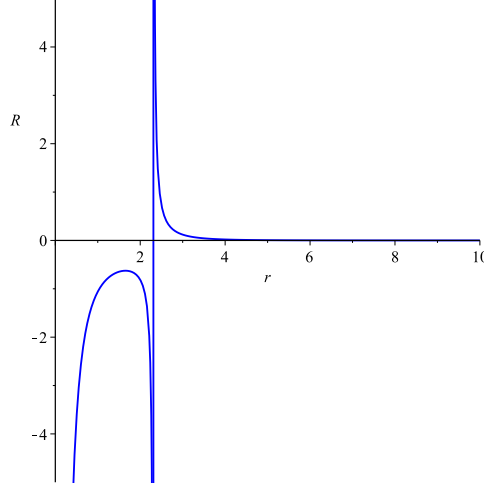


FIG. 4: Variation of Ruppeiner metric in terms of horizon radius r_+ for $l = 4.0$, $\beta = 10^{-4}$.

Plot of scalar curvature of Ruppeiner metric and heat capacity, in terms of, r_+ , have shown in Fig. 5. Also, it can be seen from Figs. 3–5, that, singular points of scalar curvature are coincide with zero point of heat capacity.

Finally, we construct the most important metric in GTD method, in which the choice of thermodynamic potential is not important, the metric for this thermodynamic system according to Eq. (4), is as follows

$$g^{GTD} = (SM_S + lM_l + \beta M_\beta) \begin{bmatrix} -M_{SS} & 0 & 0 \\ 0 & M_{ll} & 0 \\ 0 & 0 & 0 \end{bmatrix}. \quad (22)$$

We can not obtain the corresponding curvature scalar with this metric, because, the metric determinant is zero, so, inverse of the metric is infinite, therefore; in this case we can not find any physical information about the system from the GTD method.

Now, at the end of this section, we investigate the effect of changes in the value of β , and l , parameters on phase transition points. It is clear from Fig. 6, by decreasing value

of β , we do not have any changing in number of phase transition, but the place of it will decrease. In Fig. 7(a), we find that, for small value of l , the system has phase transition type one, but for the large value of l , the system is in the unstable phase and it has no phase transition (see Fig. 7(b)).

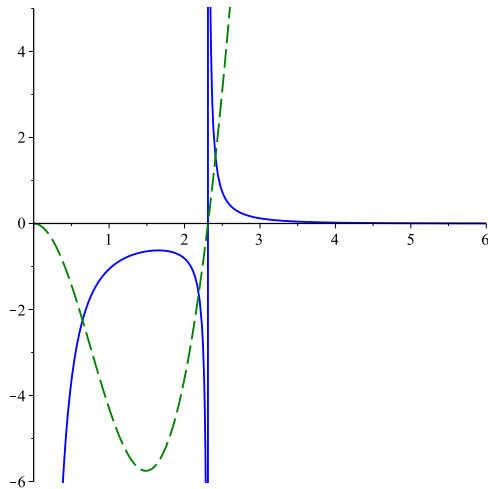


FIG. 5: Curvature scalar variation of Ruppeiner metric (blue continuous line) and the heat capacity of a static black hole (green dash line) in terms of horizon radius r_+ , for $l = 4.0$, $\beta = 10^{-4}$.

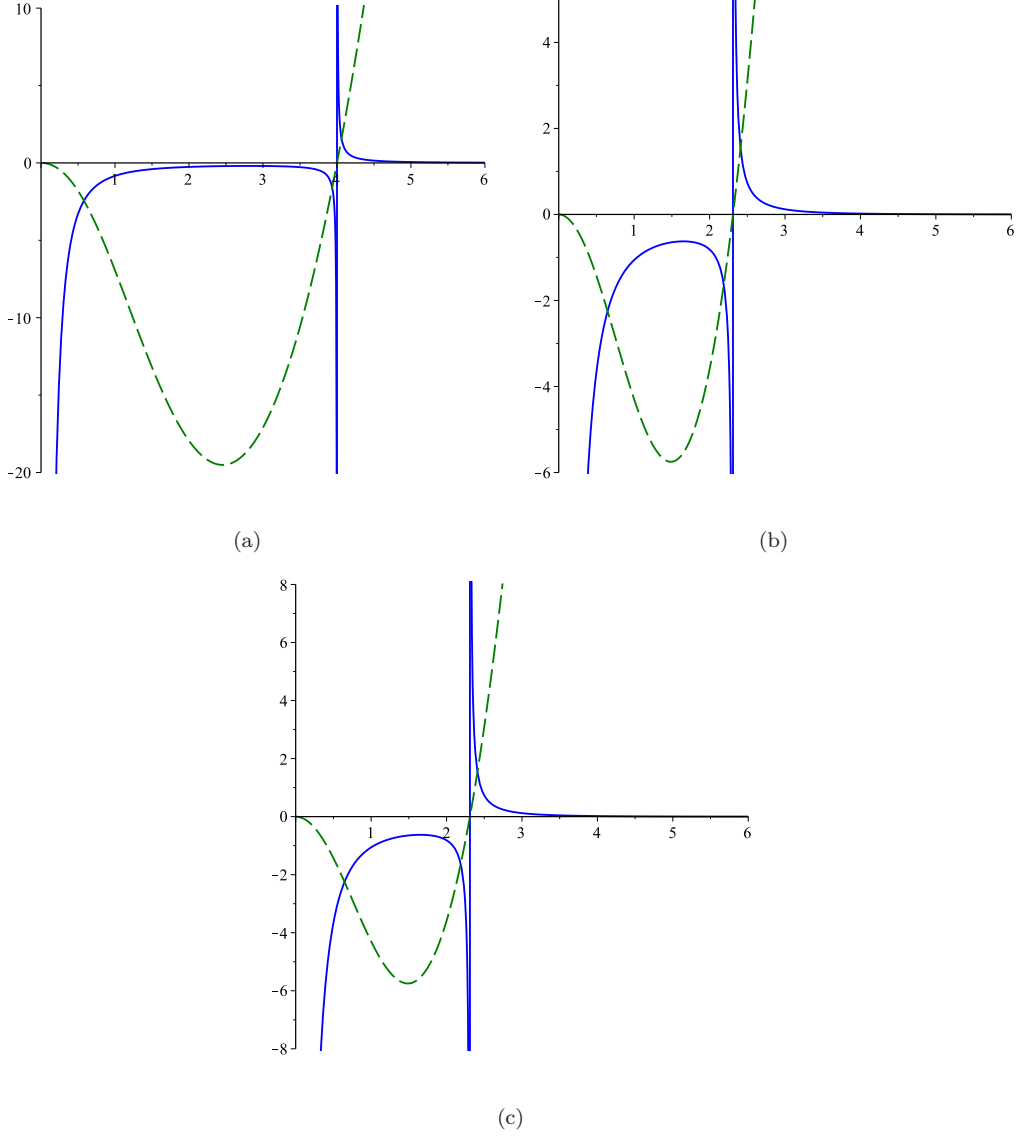


FIG. 6: Curvature scalar variation of Ruppeiner metric (blue continuous line) and the heat capacity of a static black hole (green dash line) in terms of r_+ , for $l = 4.0$ and $\beta = 0.25$, $\beta = 10^{-4}$, $\beta = 10^{-15}$, for (a), (b) and (c), respectively.

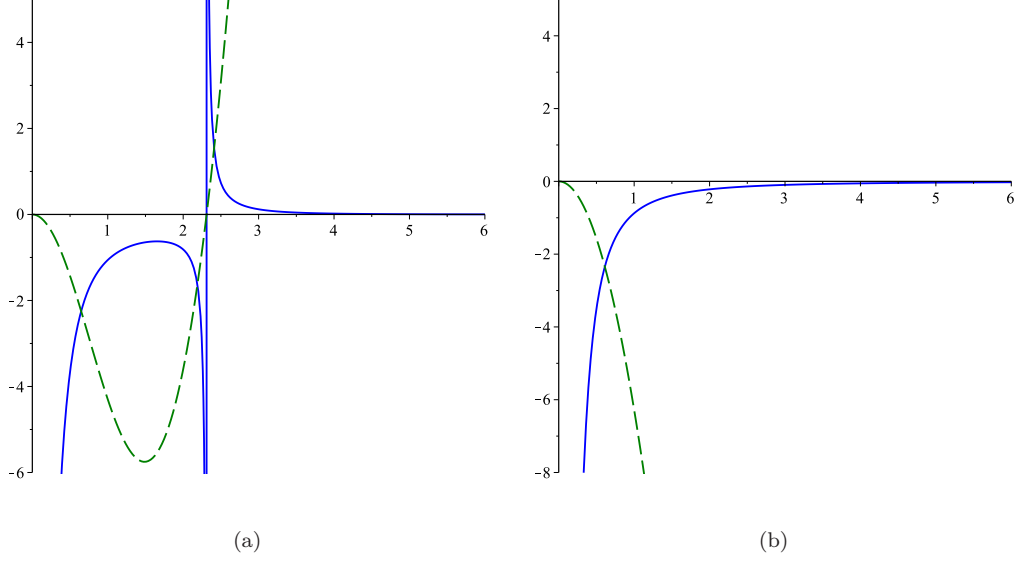


FIG. 7: Curvature scalar variation of Ruppeiner metric (blue continuous line) and the heat capacity of a static black hole (green dash line) in terms of r_+ for $\beta = 10^{-4}$, and $l = 4.0$, $l = \sqrt{3 \cdot 10^{15}}$, for (a) and (b), respectively.

In the next section, we investigate the static charged black hole in $f(R)$ gravity.

3. STATIC CHARGED BLACK HOLE IN $f(R)$ GRAVITY

In this section, we describe metric and the field equations of a static charged black hole in $f(R)$ gravity. Here, the action for $f(R)$ gravity, with Maxwell term in four dimensions, is

$$S = \frac{1}{16\pi G} \int d^4x \sqrt{-g} (R + f(R) - F_{\mu\nu} F^{\mu\nu}). \quad (23)$$

Varying the action with respect to the metric results in the field equations as:

$$R_{\mu\nu} (1 + f'(R)) - \frac{1}{2} (R + f(R)) g_{\mu\nu} + (g_{\mu\nu} \nabla^2 - \nabla_\mu \nabla_\nu) f'(R) = 2T_{\mu\nu}, \quad (24)$$

where $T_{\mu\nu}$, is the stress-energy tensor of the electromagnetic field, which is given by

$$T_{\mu\nu} = F_{\mu\rho} F_\nu^\rho - \frac{g_{\mu\nu}}{4} F_{\rho\sigma} F^{\rho\sigma}, \quad (25)$$

with

$$T^\mu_\mu = 0, \quad (26)$$

$R_{\mu\nu}$ is the Ricci tensor, and ∇ is the usual covariant derivative. The trace of Eq. (24), for $R = R_0$, yields,

$$R_0 (1 + f'(R_0)) - 2(R_0 + f(R_0)) = 0, \quad (27)$$

which determines the negative constant curvature scalar as

$$R_0 = \frac{2f(R_0)}{f'(R_0) - 1}. \quad (28)$$

Using Eqs. (24)–(28), the Ricci tensor is

$$R_{\mu\nu} = \frac{1}{2} \left(\frac{f(R_0)}{f'(R_0) - 1} \right) g_{\mu\nu} + \frac{2}{(1 + f'(R_0))} T_{\mu\nu}. \quad (29)$$

Finally, the metric of the spherically symmetric spacetime is given by

$$ds^2 = N(r)dt^2 - N(r)^{-1}dr^2 - r^2(d\theta^2 + \sin^2\theta d\varphi^2), \quad (30)$$

with

$$N(r) = 1 - \frac{2GM}{r} + \frac{Q^2}{(1 + f'(R_0))r^2} - \frac{1}{12}R_0r^2. \quad (31)$$

For a general discussion of this metric, see Ref. [29]. In the following, we consider, $G = 1$, and $q^2 = \frac{Q^2}{(1 + f'(R_0))}$, therefore we have

$$ds^2 = \left(1 - \frac{2M}{r} + \frac{q^2}{r^2} - \frac{1}{12}R_0r^2\right)dt^2 - \left(1 - \frac{2M}{r} + \frac{q^2}{r^2} - \frac{1}{12}R_0r^2\right)^{-1}dr^2 - r^2(d\theta^2 + \sin^2\theta d\varphi^2), \quad (32)$$

where $R_0 = 4\Lambda$, in which Λ is the cosmological constant, and q , is the electrical charge.

3.1. Thermodynamic

Now, in this section we investigate the thermodynamic properties of this black hole. By solving Eq.(31) in terms of r_+ ($N(r_+) = 0$) and, using the relation between entropy S , and horizon radius r_+ , the mass of this black hole will be obtained in terms of the entropy, charge and the radius of de Sitter space, as below

$$M(S, l, q) = \frac{l^2\pi^2q^2 + l^2\pi S - S^2}{2l^2\pi^{\frac{3}{2}}S^{\frac{1}{2}}}. \quad (33)$$

In following, we can straightforwardly write the temperature, the electrical potential and the heat capacity of the black hole, from the first law of thermodynamic as follows

$$dM = TdS + \Phi dq, \quad (34)$$

$$T = \frac{l^2\pi S - l^2\pi^2q^2 - 3S^2}{4l^2\pi^{\frac{3}{2}}S^{\frac{3}{2}}}, \quad (35)$$

$$\Phi = q\sqrt{\frac{\pi}{S}}, \quad (36)$$

$$C = \frac{2l^2\pi^2q^2S - 2l^2\pi S^2 + 6S^3}{-3l^2\pi^2q^2 + l^2\pi S + 3S^2}. \quad (37)$$

The plots of Eqs. (33)–(37) are demonstrated in Figs. 8–10.

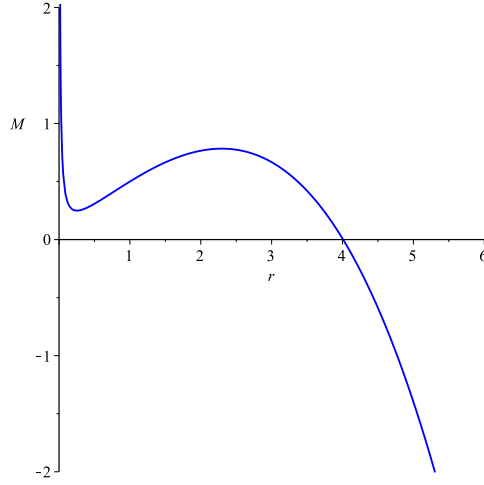


FIG. 8: Mass variation of a charged static black hole in terms of horizon radius r_+ for $q = 0.25$, $l = 4.0$.

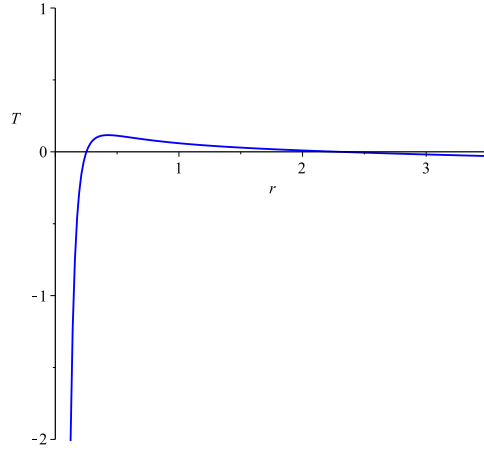


FIG. 9: Temperature variation of a charged static black hole in terms of horizon radius r_+ for $q = 0.25$, $l = 4.0$.

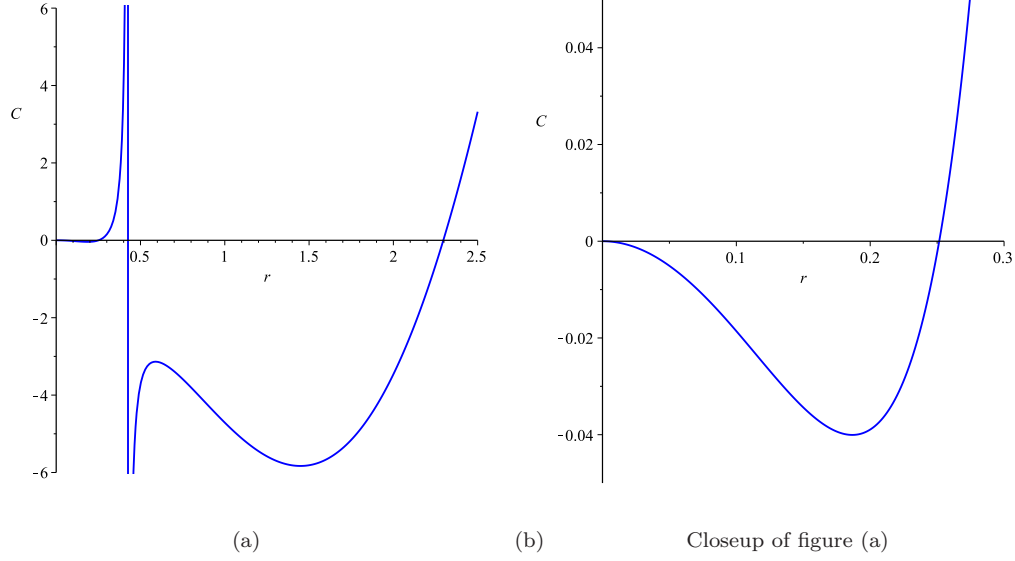


FIG. 10: Heat capacity variation of a charged static black hole in terms of horizon radius, r_+ for $l = 4.0$, $q = 0.25$.

Fig. 8, shows that, the mass of this black hole has a minimum value at $r_+ = r_{m1}$, (we show the minimum point of the mass with r_{m1}), which has the value equal to 0.252, then it reaches to its maximum value at $r_+ = r_{m2}$ (we show the maximum point of mass with r_{m2}), which its value is equal to 2.296, and it vanishes at $r = r_0$, r_0 is the point that, mass becomes zero, and it is equal to 4.0 . This is also observed from Fig. 9, that, temperature is positive only in a particular range of event horizon ($r_{m1} < r_+ < r_{m2}$), in addition, at $r_+ < r_{m1}$, and $r_{m2} < r_+$, it will be negative and, it has no physical solution. As well as, it can be observed from Fig. 10, that, the heat capacity of this black hole will be zero at r_{m1} , and r_{m2} , ($C(r_+ = r_{m1}) = 0$ and $C(r_+ = r_{m2}) = 0$), in the other words, it has two phase transition type one at these points, moreover, at $r_+ = r_\infty$ (we show the divergence point of heat capacity with r_∞), heat capacity diverges, that, the value of this point is equal to 0.426. In other words, at $r_+ < r_{m1}$, heat capacity is negative and it is in unstable phase, then, at $r_{m1} < r_+ < r_\infty$, heat capacity is positive or it is in stable phase, afterward, at $r_\infty < r_+ < r_{m2}$, it falls in to negative region (unstable phase) and, at $r_+ > r_{m2}$, it becomes stable.

3.2. Thermodynamic Geometry

In this section, we construct the thermodynamic geometry structure for this black hole. First, we use Weinhold method. Extensive variables for this system are $N^r = (l, q)$, so the

resulting matrix of the Weinhold metric becomes

$$g^W = \begin{bmatrix} M_{SS} & M_{Sq} & M_{Sl} \\ M_{qS} & M_{qq} & 0 \\ M_{lS} & 0 & M_{ll} \end{bmatrix}. \quad (38)$$

The elements of the metric can be obtained from the Eq. (33), and Weinhold scalar curvature can be found as

$$R^W = \frac{9l^2\pi^{\frac{3}{2}}S^{\frac{5}{2}} - l^4\pi^{\frac{7}{2}}q^2S^{\frac{1}{2}} - l^4\pi^{\frac{5}{2}}S^{\frac{3}{2}}}{(l^2\pi^2q^2 - l^2\pi S + 3S^2)^2}. \quad (39)$$

Denominator of the above expression becomes zero at $S = \frac{\pi l}{6}(l \pm \sqrt{l^2 - 12q^2})$, or at $r_+ = r_{m1}$, and $r_+ = r_{m2}$, (see, Fig. 11).

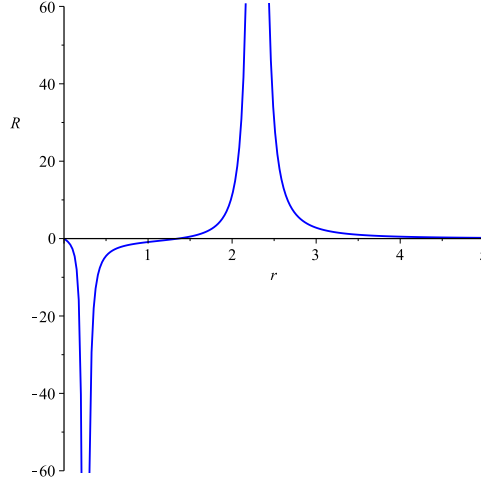


FIG. 11: Curvature scalar variation of the Weinhold metric in terms of horizon radius r_+ for $l = 4.0$, $q = 0.25$.

Next, we use the Ruppeiner method for this black hole. Using Eq. (33), matrix components of Ruppeiner metric will be obtained as

$$g^R = \frac{1}{T} \begin{bmatrix} M_{SS} & M_{Sq} & M_{Sl} \\ M_{qS} & M_{qq} & 0 \\ M_{lS} & 0 & M_{ll} \end{bmatrix}. \quad (40)$$

So, using Eqs. (35) and (40), we obtain

$$g^R = \frac{4l^2\pi^{\frac{3}{2}}S^{\frac{3}{2}}}{l^2\pi S - l^2\pi^2q^2 - 3S^2} \begin{bmatrix} M_{SS} & M_{Sq} & M_{Sl} \\ M_{qS} & M_{qq} & 0 \\ M_{lS} & 0 & M_{ll} \end{bmatrix}. \quad (41)$$

After some calculation, the corresponding curvature scalar will be obtained as

$$R^R = -\frac{l^2\pi(2\pi q^2 - S)}{S(l^2\pi^2q^2 - l^2\pi S + 3S^2)}, \quad (42)$$

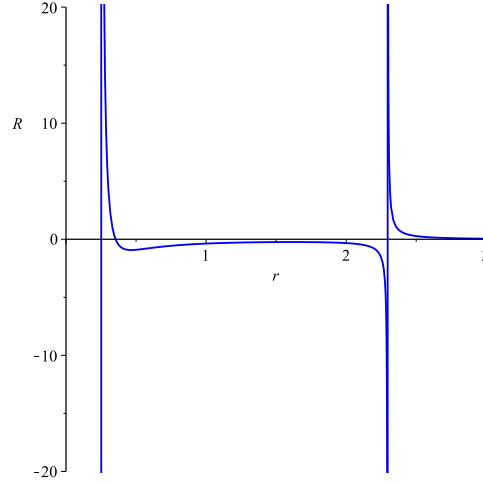


FIG. 12: Curvature scalar variation of the Ruppeiner metric in terms of horizon radius r_+ for $l = 4.0$, $q = 0.25$.

This curvature scalar is singular at $S = 0$ and $S = \frac{\pi l}{6}(l \pm \sqrt{l^2 - 12q^2})$, or as it can be seen from Fig. 12, it is singular at $r_+ = 0$, $r_+ = r_{m1}$ and $r_+ = r_{m2}$.

Finally, we use the most important GTD metric. The resulting matrix from the metric is as follows

$$g^{GTD} = (SM_S + qM_q + lM_l) \begin{bmatrix} -M_{SS} & 0 & 0 \\ 0 & M_{qq} & 0 \\ 0 & 0 & M_{ll} \end{bmatrix}. \quad (43)$$

The corresponding curvature scalar will be obtained as

$$R^{GTD} = \frac{16}{3} \frac{\mathcal{N}}{(3l^2\pi^2q^2 - l^2\pi S - 3S^2)^2(3l^2\pi^2q^2 + l^2\pi S + S^2)^3}. \quad (44)$$

Where, because the numerator of the above expression has no physical information and it is too long, so, we consider it as \mathcal{N} . The denominator of R^{GTD} , becomes zero at $r_+ = r_\infty$, (see Fig. 13). So, we extended our study to different thermodynamical geometry. It can be observed from Fig. 14, that, Weinhold and Ruppeiner methods are compatible with zeros of the heat capacity, and GTD method is coincide with divergences of it. In following, we point out the effect of different values of spacetime parameters on stability conditions of this black hole. As, it can be seen from Fig. 15(a), for $q = 0$, the heat capacity of this black hole treats like the black hole in previous section and It has only one phase transition type one. By increasing the value of q , it will have two phase transition type one and one phase transition type two. Also, for small value of l , heat capacity has two phase transition type one and one phase transition type two (see, Fig. 16(a,b)), and for large value of l , it has one phase transition type one and one phase transition type two (see, Fig. 16(c,d)).

In the next section, we study thermodynamic behavior of a rotating charged black hole in $f(R)$ gravity.

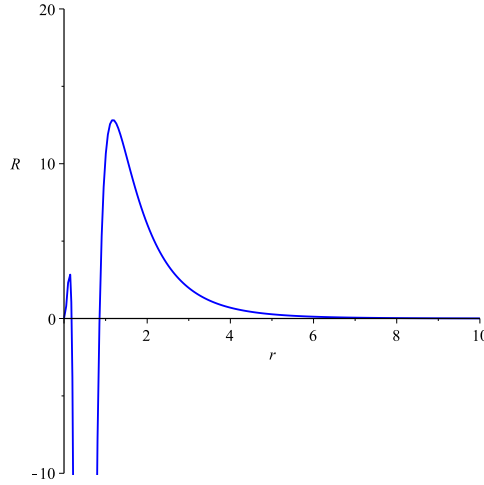


FIG. 13: Curvature scalar variation of GTD metric in terms of horizon radius r_+ for $l = 4.0$, $q = 0.25$.

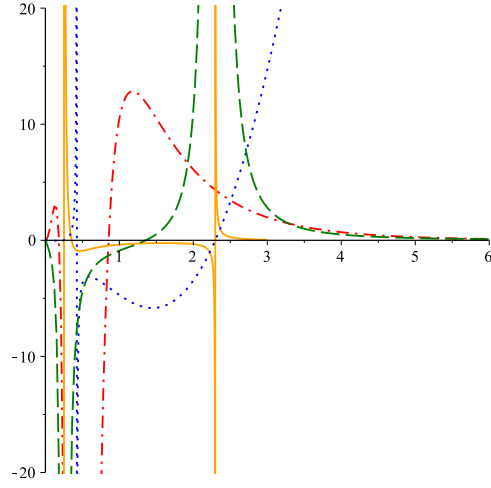


FIG. 14: curvature scalar variation of GTD (red dash-dot line), Ruppeiner (orange continuous line), Weinhold (green dash line) metrics, and the heat capacity (blue dot line), in terms of horizon radius r_+ , for $l = 4.0$, $q = 0.25$.

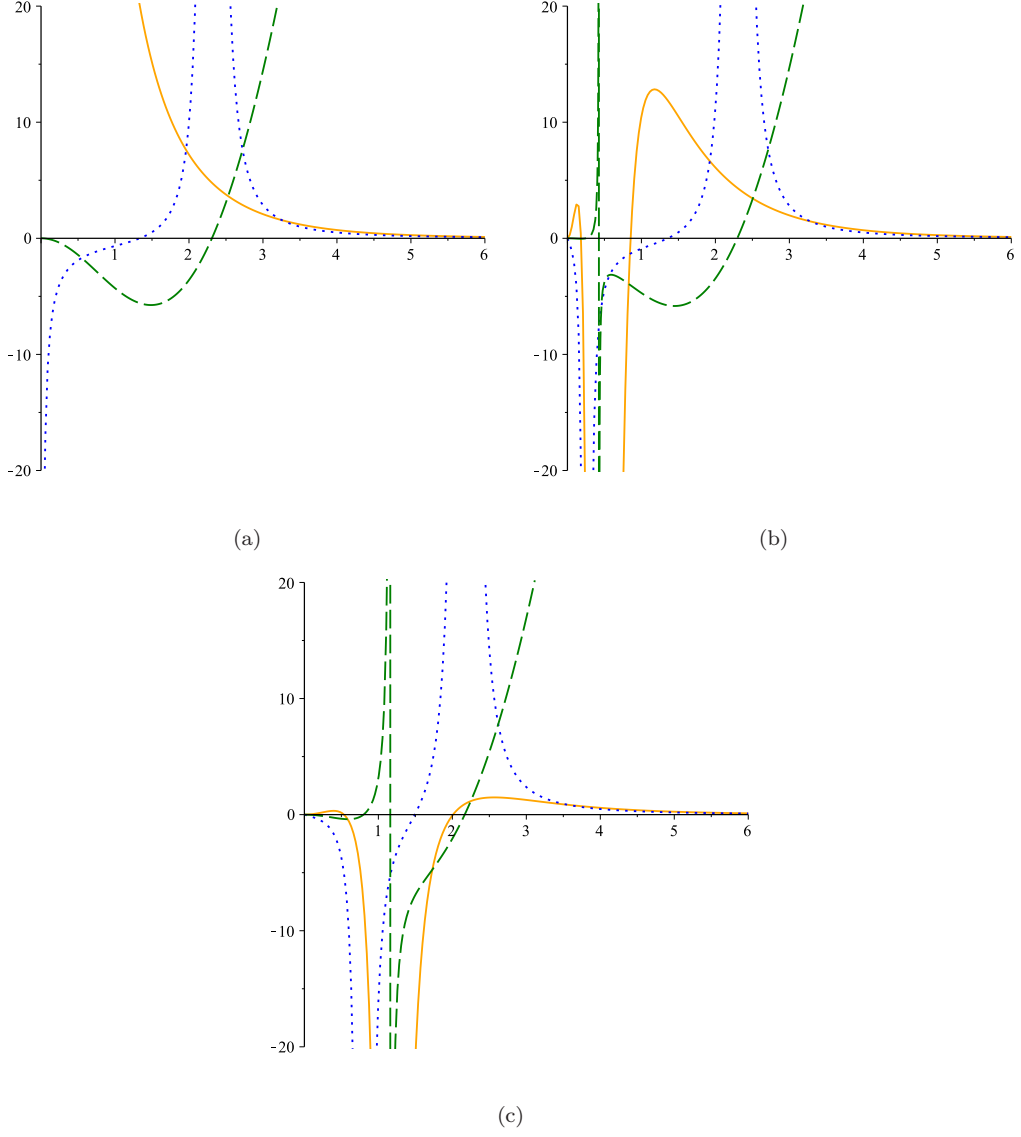


FIG. 15: Curvature scalar variation of GTD (orange continuous line), Weinhold (blue dot line) metrics, and the heat capacity (green dash line) in terms of r_+ , for $l = 4.0$ and $q = 0$, $q = 0.25$, $q = 0.75$, for (a), (b) and (c), respectively.

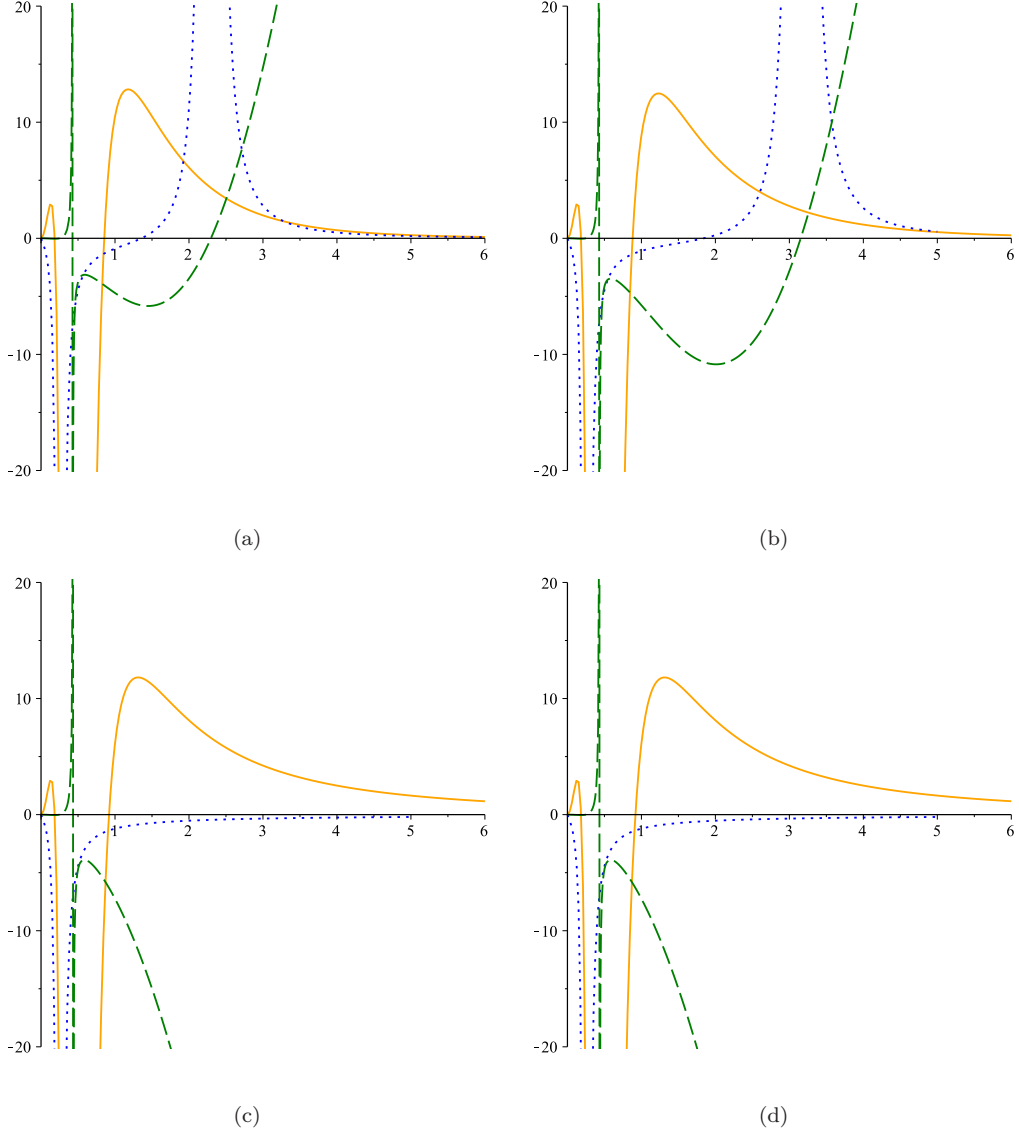


FIG. 16: Curvature scalar variation of GTD (orange continuous line), Weinhold (blue dot line) metrics, and the heat capacity (green dash line) in terms of r_+ , for $q = 0.25$ and $l = 4.0$, $l = \sqrt{30}$, $l = \sqrt{3} \cdot 10^4$, $l = \sqrt{3} \cdot 10^{15}$, for (a), (b), (c) and (d), respectively.

4. ROTATING CHARGED BLACK HOLE IN $f(R)$ GRAVITY

In this section, we study solution of the field equation and metric of a rotating charged black hole in $f(R)$ gravity. With Maxwell term in four dimensions, the action is

$$S = S_g + S_M, \quad (45)$$

where, S_g , is the gravitational action as

$$S_g = \frac{1}{16\pi} \int d^D x \sqrt{|g|} (R + f(R)), \quad (46)$$

and S_M , is the electromagnetic actions as

$$S_M = \frac{-1}{16\pi} \int d^4 x \sqrt{-g} [F_{\mu\nu} F^{\mu\nu}], \quad (47)$$

where, R , is the scalar curvature and $R + f(R)$, is the function defining the theory under consideration, and g , is the determinant of the metric. From the Eq. (47), the Maxwell equation takes the form

$$\nabla_\mu F^{\mu\nu} = 0. \quad (48)$$

The field equations in the metric formalism are [30]

$$R_{\mu\nu} (1 + f'(R)) - \frac{1}{2} (R + f(R)) g_{\mu\nu} + (g_{\mu\nu} \nabla^2 - \nabla_\mu \nabla_\nu) f'(R) = 2T_{\mu\nu}, \quad (49)$$

where ∇ is the usual covariant derivative, $R_{\mu\nu}$, is the Ricci tensor and $T_{\mu\nu}$, the stress-energy tensor of the electromagnetic field as

$$T_{\mu\nu} = F_{\mu\rho} F_\nu^\rho - \frac{g_{\mu\nu}}{4} F_{\rho\sigma} F^{\rho\sigma}, \quad (50)$$

with

$$T^\mu_\mu = 0. \quad (51)$$

The trace of Eq. (49) with the constant curvature scalar $R = R_0$, yields

$$R_0 (1 + f'(R_0)) - 2(R_0 + f(R_0)) = 0, \quad (52)$$

which determines the negative constant curvature scalar as

$$R_0 = \frac{2f(R_0)}{f'(R_0) - 1}. \quad (53)$$

Using Eqs. (49)–(53), we have

$$R_{\mu\nu} = \frac{1}{2} \left(\frac{f(R_0)}{f'(R_0) - 1} \right) g_{\mu\nu} + \frac{2}{(1 + f'(R_0))} T_{\mu\nu}. \quad (54)$$

Finally, the axisymmetric ansatz in Boyer–Lindquist-type coordinates (t, r, θ, φ) , inspired by the Kerr-Newman-AdS black hole solution, is [30]

$$ds^2 = -\frac{\Delta_r}{\rho^2} \left[dt - \frac{a \sin^2 \theta d\varphi}{\Xi} \right]^2 + \frac{\rho^2}{\Delta_r} dr^2 + \frac{\rho^2}{\Delta_\theta} d\theta^2 + \frac{\Delta_\theta \sin^2 \theta}{\rho^2} \left[a dt - \frac{r^2 + a^2}{\Xi} d\varphi \right]^2, \quad (55)$$

where

$$\Delta_r = (r^2 + a^2) \left(1 + \frac{R_0}{12} r^2 \right) - 2mr + \frac{Q^2}{(1 + f'(R_0))}, \quad (56)$$

$$\Xi = 1 - \frac{R_0}{12} a^2, \quad \rho^2 = r^2 + a^2 \cos^2 \theta, \quad \Delta_\theta = 1 - \frac{R_0}{12} a^2 \cos^2 \theta, \quad (57)$$

in which R_0 , is a constant proper to cosmological constant ($R_0 = -4\Lambda$), Q , is the electric charge and a , is the angular momentum per mass of the black hole.

4.1. Thermodynamic

In this section, we investigate the thermodynamic peroperties of this black hole. The radius of the horizon (r_+) satisfy the condition $\Delta_r = 0$,

$$(r_+^2 + a^2) \left(1 + \frac{R_0}{12} r_+^2 \right) - 2mr_+ + \frac{Q^2}{(1 + f'(R_0))} = 0. \quad (58)$$

By setting $dr = dt = 0$, in the metric line elements, we can find line elements for the 2-Dimensional horizon. Using the relation

$$A = \int_0^{2\pi} d\varphi \int_0^\pi \sqrt{|\gamma|} d\theta, \quad (59)$$

where γ , is the metric tensor of the black hole horizon, the area of this black hole will be obtained as

$$A = \frac{4\pi(r_+^2 + a^2)}{1 - \frac{R_0}{12} a^2}. \quad (60)$$

According to relation for entropy, $S = \frac{A}{4}$ [2], we can easily find the entropy of this black hole as,

$$S = \frac{\pi(r_+^2 + a^2)}{1 - \frac{R_0}{12}a^2}. \quad (61)$$

Mass of the black hole can be obtained by using generalized Smarr formula in terms of all its parameter. To calculate generalized Smarr formula, first we obtain total mass (M), and angular momentum (J), by means of Kommar integrals and using the killing vectors, $\frac{1}{\Xi}\partial_t$, and ∂_φ , so they will be obtained as

$$M = \frac{m}{\Xi^2}, \quad (62)$$

$$J = \frac{am}{\Xi^2}. \quad (63)$$

Using Eqs. (58)–(63), the generalized Smarr formula will be obtained as

$$M^2 = \frac{S}{4\pi} + \frac{\pi}{4S} [4J^2 + q^4] + \frac{q^2}{2} - \frac{R_0}{12}J^2 - \frac{R_0S}{24\pi} \left[q^2 + \frac{S}{\pi} - \frac{R_0S^2}{24\pi^2} \right]. \quad (64)$$

Now, according to the first law of thermodynamic, we can calculate all of the thermodynamic quantities,

$$dM = TdS + \Omega dJ + \Phi dq. \quad (65)$$

So, the temperature of this black hole is,

$$\begin{aligned} T = \frac{\partial M}{\partial S} = & -(48q^4\pi^5 + 8R_0\pi^3R_0S^2q^2 + 192\pi^5J^2 - R_0^2\pi S^4 + 16R_0\pi^2S^3 - 48\pi^3S^2) \cdot \\ & (256\pi^4S^3(144\pi^5q^4 - 48R_0\pi^4J^2S - 24R_0\pi^3q^2S^2 + 576\pi^5J^2 + \\ & 288\pi^4q^2S + R_0^2\pi S^4 - 24R_0\pi^2S^3 + 144\pi^3S^2))^{-\frac{1}{2}}, \end{aligned} \quad (66)$$

In addition, the angular velocity Ω is,

$$\begin{aligned} \Omega = \frac{\partial M}{\partial J} = & -(2\pi^2J(R_0S - 12\pi)) \cdot (S(144\pi^5q^4 - 48R_0\pi^4J^2S - 24R_0\pi^3q^2S^2 + 576\pi^5J^2 + \\ & 288\pi^4q^2S + R_0^2\pi S^4 - 24R_0\pi^2S^3 + 144\pi^3S^2))^{-\frac{1}{2}}, \end{aligned} \quad (67)$$

and, also the electrical potential can be obtained as,

$$\Phi = \frac{\partial M}{\partial q} = -\pi q(-12\pi^2 q^2 + R_0 S^2 - 12\pi S) \cdot (S(144\pi^5 q^4 - 48R_0\pi^4 J^2 S - 24R_0\pi^3 q^2 S^2 + 576\pi^5 J^2 + 288\pi^4 q^2 S + R_0^2\pi S^4 - 24R_0\pi^2 S^3 + 144\pi^3 S^2))^{-\frac{1}{2}}. \quad (68)$$

Finally, we can calculate the heat capacity of this black hole as follows

$$C = \frac{\partial_S M}{\partial_S^2 M}. \quad (69)$$

Plot of all thermodynamic parameters obtained for this black hole, are shown in Figs. 17-19.

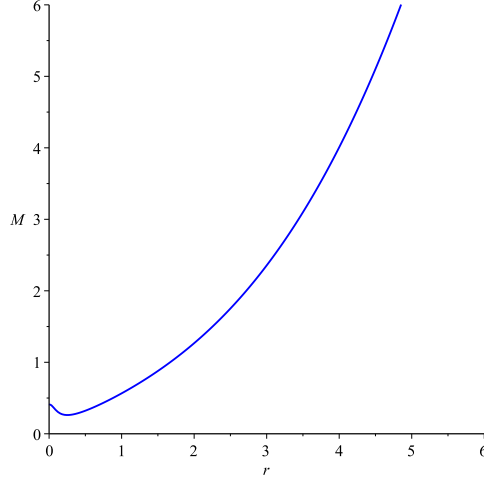


FIG. 17: Mass variation of a Rotating charged black hole in terms of its horizon radius r_+ for $l = 4.0$, $a = 0.1$, $q = 0.25$.

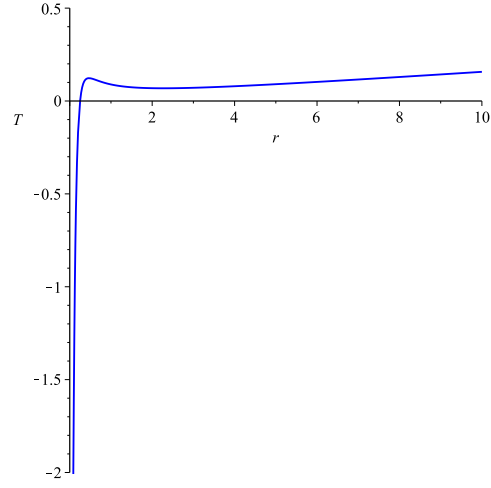


FIG. 18: Temperature variation of a Rotating charged black hole in terms of its horizon radius r_+ for $l = 4.0$, $a = 0.1$, $q = 0.25$.

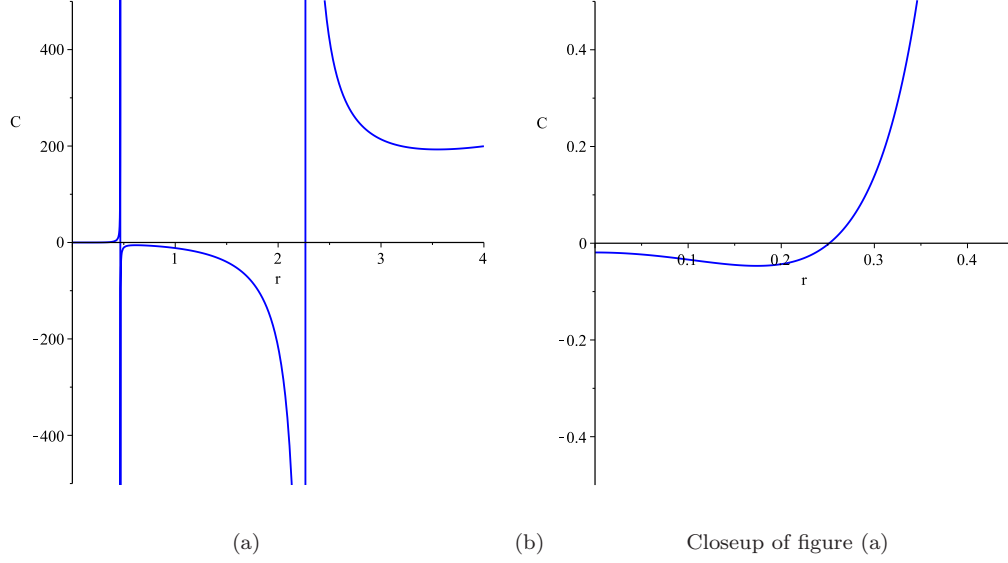


FIG. 19: Heat capacity variation of a Rotating charged black hole in terms of horizon radius r_+ , for $l = 4.0$, $a = 0.1$, $q = 0.25$.

It can be seen from Fig. 17, the mass of this black hole, has one minimum point at $r_+ = r_m$, (we show the place of minimum point of the mass with r_m), in which the value of it, is equal to 0.252. It is also observed from the plot of temperature in Fig. 18, that, the temperature of this system is in the negative region at a particular range of r_+ ($r_+ < r_m$), after that, it reaches to zero at $r_+ = r_m$, then, it will be positive for $r_+ > r_m$. In addition, Fig. 19, shows that, the heat capacity of this black hole arrives to positive (stable) phase from negative (unstable) phase, after that, it reaches to zero at $r_+ = r_m$. Also the divergence points of heat capacity are $r_{\infty 1}$ and $r_{\infty 2}$, that, for this system $r_{\infty 1} = 0.466$ and $r_{\infty 2} = 2.266$. So, for the range of $r_m < r_+ < r_{\infty 1}$, the heat capacity is positive and system is in the stable phase, after that, at $r_{\infty 1} < r_+ < r_{\infty 2}$, it falls in to negative region (unstable phase), then at $r_+ > r_{\infty 2}$ it will be positive(stable). In other words, the heat capacity of this black hole, has one phase transition type one, and two phase transition type two.

4.2. Thermodynamic geometry

In this part, we investigate thermodynamic geometry of this black hole, using Weinhold, Ruppeiner and GTD methods. We start by Weinhold metric, which is as follows

$$g^W = \begin{bmatrix} M_{SS} & M_{SJ} & M_{Sq} & M_{Sl} \\ M_{JS} & M_{JJ} & M_{Jq} & M_{Jl} \\ M_{qS} & M_{qJ} & M_{qq} & M_{lq} \\ M_{lS} & M_{lJ} & M_{lq} & M_{ll} \end{bmatrix}. \quad (70)$$

The scalar curvature R^W , can be easily obtained, which is plotted in Fig. 20.

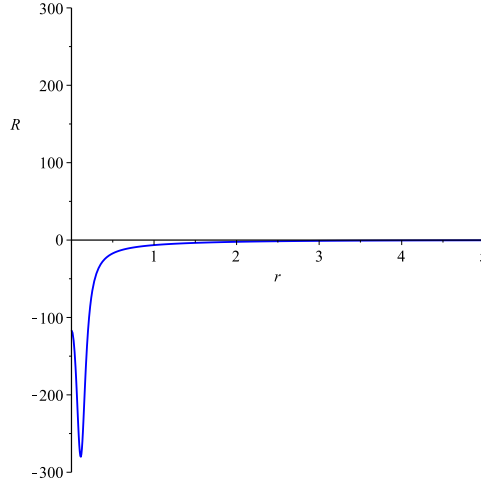


FIG. 20: Curvature scalar variation of Weinhold metric in terms of horizon radius r_+ for $l = 4.0$, $q = 0.25$, $a = 0.1$.

It can be seen from Fig. 20, The curvature scalar has no singularity, so Weinhold method has no physical information for this system.

Now, we construct Ruppeiner metric for this black hole as follows

$$g^R = \frac{1}{T} \begin{bmatrix} M_{SS} & M_{SJ} & M_{Sq} & M_{Sl} \\ M_{JS} & M_{JJ} & M_{Jq} & M_{Jl} \\ M_{qS} & M_{qJ} & M_{qq} & M_{lq} \\ M_{lS} & M_{lJ} & M_{lq} & M_{ll} \end{bmatrix}, \quad (71)$$

where, T , can be obtained from Eq. (66). The curvature scalar, which is correspond to above metric, is plotted in Fig. 21, and it is singular at $r_+ = r_m$.

Finally, at the end of this section, we apply the most important metric of GTD method to this thermodynamic system, as

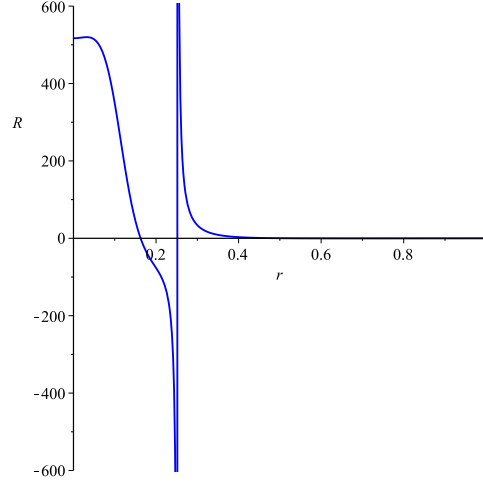


FIG. 21: Curvature scalar variation of Ruppeiner metric in terms of horizon radius r_+ . $l = 4.0$ for $q = 0.25$, $a = 0.1$.

$$g^{GTD} = \begin{bmatrix} -M_{SS} & 0 & 0 & 0 \\ 0 & M_{JJ} & M_{Jq} & M_{Jl} \\ 0 & M_{qJ} & M_{qq} & M_{lq} \\ 0 & M_{lJ} & M_{lq} & M_{ll} \end{bmatrix}. \quad (72)$$

Plot of the corresponding curvature scalar with GTD metric, is shown in Fig. 22.

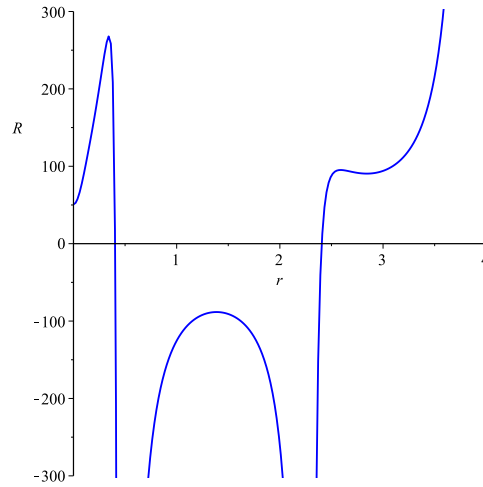


FIG. 22: Curvature scalar variation of GTD metric in terms of horizon radius r_+ for $l = 4.0$, $a = 0.1$ and $q = 0.25$.

This curvature scalar is singular at $r_+ = r_{\infty 1}$ and $r_+ = r_{\infty 2}$. So, again we extended our study to different geothermodynamic methods, and our results are shown in Fig. 23. It can be observed from Fig. 23, singularities of Ruppeiner metric is compatible with the zero

point of heat capacity, and singularities of GTD metric, are coincide with divergence points of heat capacity. At the end of this section, we investigate the effect of different values of q , a , and l , parameters on phase transition points for this system.

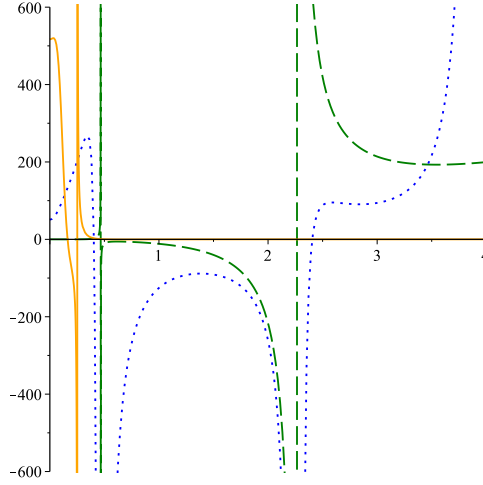


FIG. 23: Curvature scalar variation of Ruppeiner (orange continuous line), GTD (blue dot line) metrics, and the heat capacity (green dash line) of a rotating black hole in terms of r_+ for $l = 4.0$, $a = 0.1$, $q = 0.25$.

In Figs. 24–26, we plot curvature scalar of Ruppeiner and GTD metrics with the heat capacity of this black hole. It can be seen from Figs. 24(a), 25(a) and 26(a), that, this thermodynamical system has one phase transition type one and two phase transition type two. The number of these phase transitions changes for different value of q , a and l , parameters. By increasing the value of q , the number of phase transitions will be decreased, as it can be observed from Fig. 24(c,d), it has only one phase transition type one. Also, by increasing the value of a , the number of phase transitions will be decreased, as it shown in Fig. 25(d), it has two phase transition type two. Moreover, By increasing the value of l , the number of phase transitions will be decreased, and it has only one phase transition type two (see Fig. 26(c,d)).

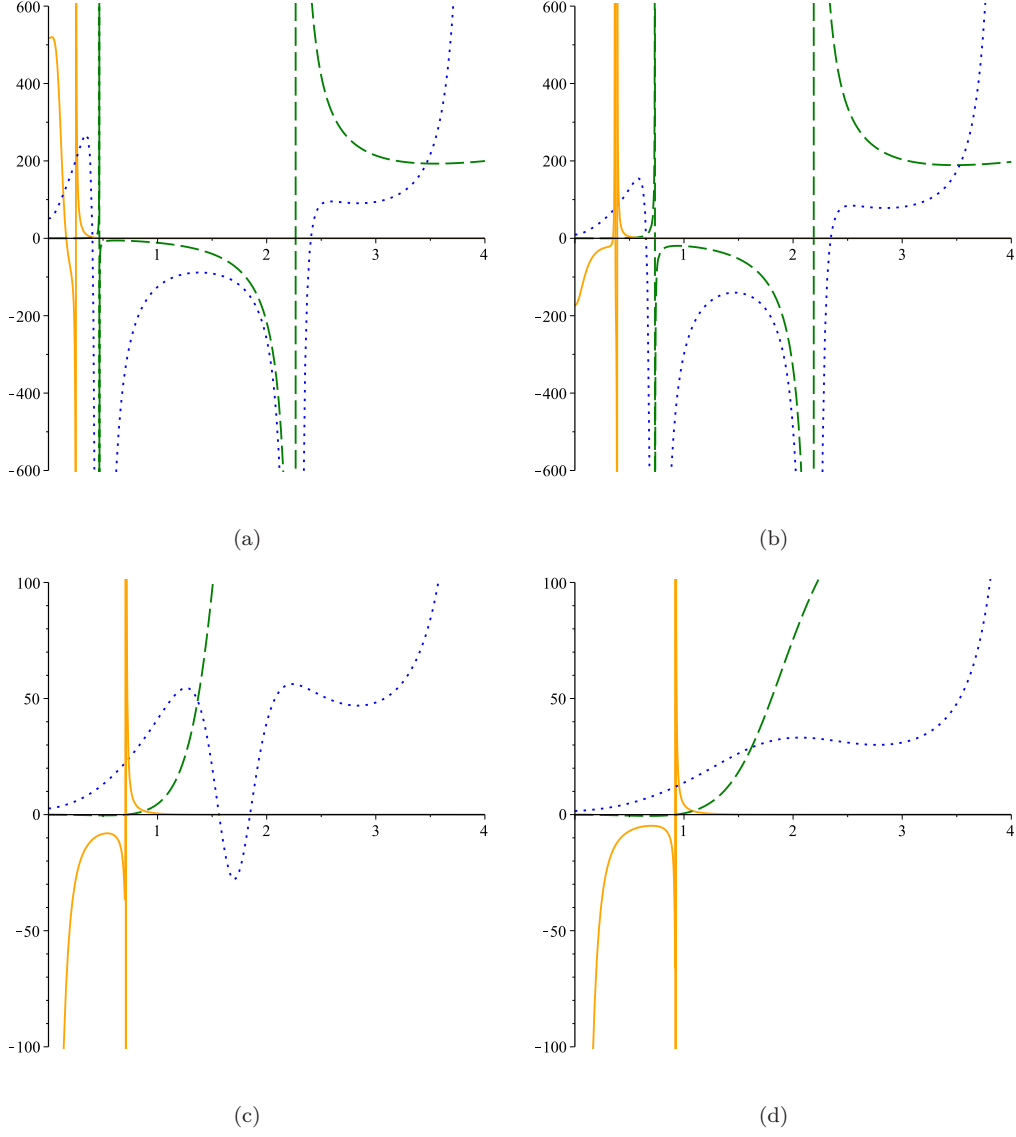


FIG. 24: Curvature scalar variation of Ruppeiner (orange continuous line), GTD (blue dot line) metrics and the heat capacity (green dash line) of a rotating black hole in terms of r_+ for $l = 4.0$, $a = 0.1$ and $q = 0.25$, $q = 0.4$, $q = 0.75$, $q = 1$, for (a), (b), (c) and (d), respectively.

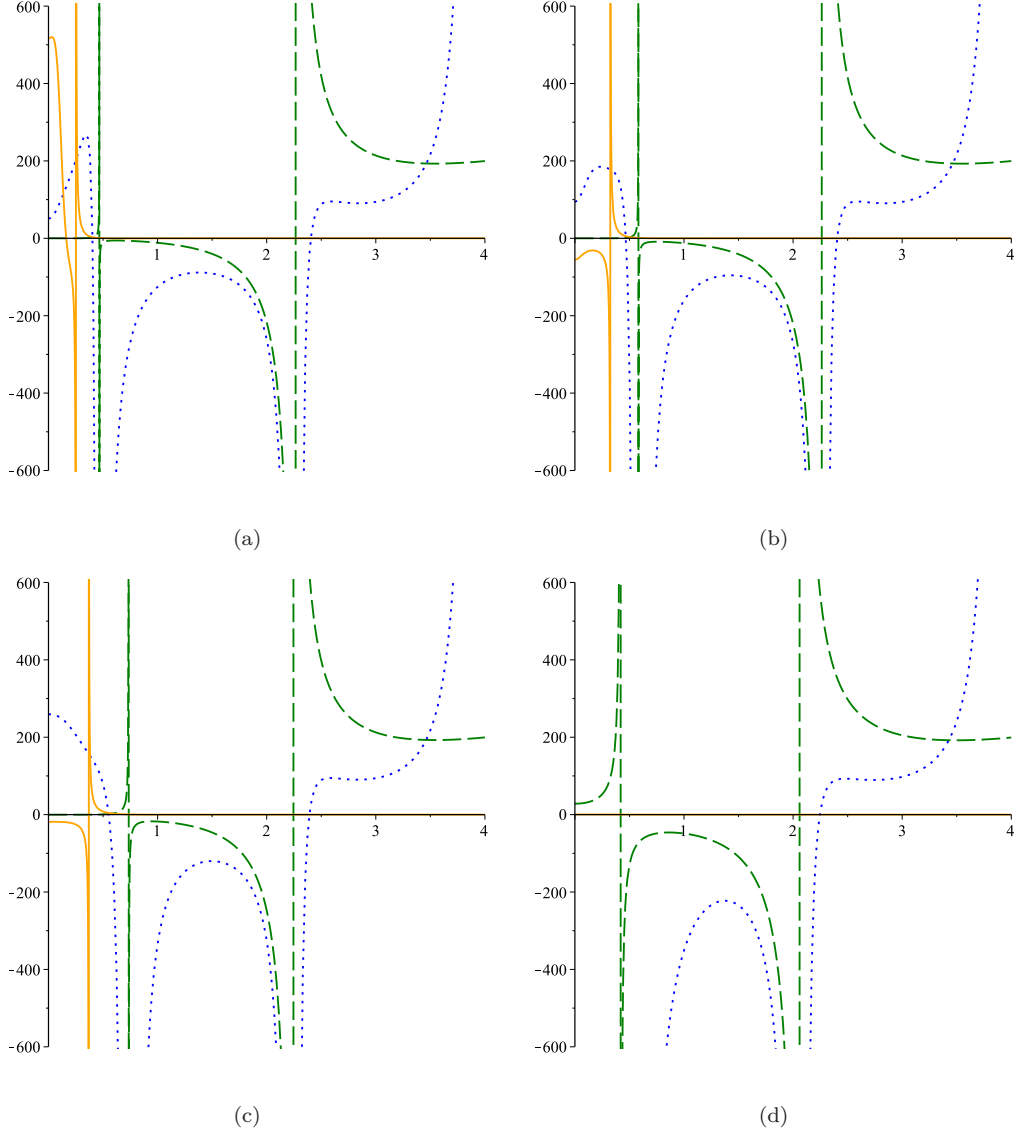


FIG. 25: Curvature scalar variation of Ruppeiner (orange continuous line), GTD (blue dot line) metrics, and the heat capacity (green dash line) of a rotating black hole in terms of r_+ for $l = 4.0$, $q = 0.25$ and $a = 0.1$, $a = 0.25$, $a = 0.5$, $a = 0.8$, for (a), (b), (c) and (d), respectively.

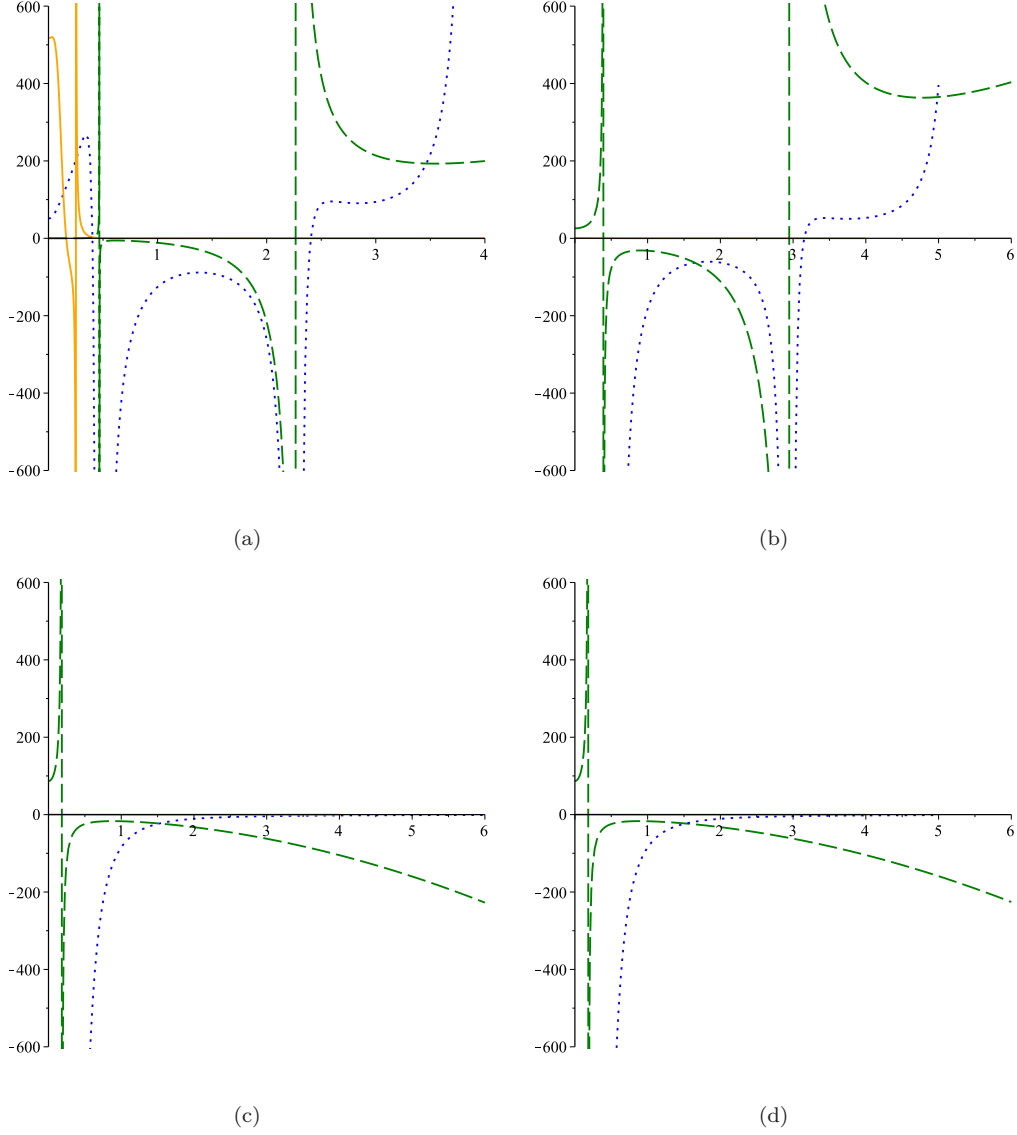


FIG. 26: Curvature scalar variation of Ruppeiner (orange continuous line), GTD (blue dot line) metrics, and the heat capacity (green dash line) of a rotating black hole in terms of r_+ for $q = 0.25$, $a = 0.1$ and $l = 4.0$, $l = \sqrt{30}$, $l = \sqrt{3} \cdot 10^4$, $l = \sqrt{3} \cdot 10^{15}$, for (a), (b), (c) and (d), respectively.

5. CONCLUSION

In this paper, we studied thermodynamic behavior of three types (static, charged static and charged rotating) of black holes in $f(R)$ gravity, and investigated the thermodynamic geometry of them. Also, we plotted thermodynamic quantities in terms of horizon radius r_+ and, we showed that for each maximum and minimum value of mass, these black holes have one zero point in their temperature and heat capacity. When we applied the thermodynamic

geometry methods to these black holes, we have seen that, for static black hole, Weinhold metric is flat, and Ruppeiner metric can explain the zero points of it. For the static charged black hole, Weinhold and Ruppeiner metrics coincide with the zero points of heat capacity, and GTD metric can explain the divergence point of it, as well. Moreover, for the rotating charged black hole, Weinhold metric has no singularity, but, Ruppeiner metric can explain the zero points of heat capacity and GTD metric coincides with divergence point of it.

We also, investigated the effects of different values of spacetime parameters on stability conditions of these black holes. We observed that, by changing in value of spacetime parameters, the number of phase transitions of these black holes is changed. But these changes has not affected on compatibility of explained thermodynamical geometry methods with zeros and divergence points of heat capacity.

For future work, it would be interesting to apply these methods to other spacetimes such as dilaton black holes.

-
- [1] S. W. Hawking, *Nature* **248** (1974) 30.
 - [2] J. D. Bekenstein, *Phys. Rev. D* **7** (1973) 2333.
 - [3] S. W. Hawking, *Commun. Math. Phys.* **43**, 199 (1975) Erratum: [*Commun. Math. Phys.* **46**, 206 (1976)].
 - [4] D. Kothawala, T. Padmanabhan and S. Sarkar, *Phys. Rev. D* **78**, 104018 (2008) [arXiv:0807.1481 [gr-qc]].
 - [5] T. Padmanabhan, *Class. Quant. Grav.* **21**, 4485 (2004) [gr-qc/0308070].
 - [6] J. D. Bekenstein, *Lett. Nuovo Cim.* **4**, 737 (1972).
 - [7] Y. S. Myung, *Phys. Rev. D* **77**, 104007 (2008) [arXiv:0712.3315 [gr-qc]]. B. M. N. Carter and I. P. Neupane, *Phys. Rev. D* **72**, 043534 (2005) [gr-qc/0506103]. D. Kastor, S. Ray and J. Traschen, *Class. Quant. Grav.* **26**, 195011 (2009) [arXiv:0904.2765 [hep-th]]. F. Capela and G. Nardini, *Phys. Rev. D* **86**, 024030 (2012) [arXiv:1203.4222 [gr-qc]].
 - [8] R. Hermann., *Geometry, physics and systems*, (Marcel Dekker., New York, 1973).
 - [9] F. Weinhold, *J. Chem. Phys* **63**, 2479 (1975).
 - [10] G. Ruppeiner, *Phys. Rev. A* **20**, 1608 (1979).
 - [11] R. Mrugala, *Physica. A* (Amsterdam), **125**, 631 (1984).

- [12] P. Salamon, J. D. Nulton and E. Ihrig, J. Chem. Phys, **80**,436 (1984).
- [13] H. Quevedo, J. Math. Phys. **48** (2007) 013506 [physics/0604164].
- [14] H. Quevedo, Gen. Rel. Grav. **40**, 971 (2008) [arXiv:0704.3102 [gr-qc]].
- [15] H. Weyl, Annalen Phys. **59**, 101 (1919) [Surveys High Energ. Phys. **5**, 237 (1986)] [Annalen Phys. **364**, 101 (1919)].
- [16] Eddington, A. S., *The Mathematical Theory of Relativity*, (Cambridge University Press, Cambridge, 1923).
- [17] C. Brans and R. H. Dicke, Phys. Rev. **124**, 925 (1961).
- [18] A. G. Riess *et al.* [Supernova Search Team Collaboration], Astron. J. **116**, 1009 (1998) [astro-ph/9805201]. S. Perlmutter *et al.* [Supernova Cosmology Project Collaboration], Astrophys. J. **517**, 565 (1999) [astro-ph/9812133]. J. L. Tonry *et al.* [Supernova Search Team Collaboration], Astrophys. J. **594**, 1 (2003) [astro-ph/0305008]. C. L. Bennett *et al.* [WMAP Collaboration], Astrophys. J. Suppl. **148**, 1 (2003) [astro-ph/0302207]. G. Hinshaw *et al.* [WMAP Collaboration], Astrophys. J. Suppl. **170**, 288 (2007) [astro-ph/0603451].
- [19] Y. Fujii and K. Maeda. *The Scalar-Tensor Theory of Gravitation* (Cambridge University Press, Cambridge, 2003). T. P. Sotiriou, Class. Quant. Grav. **23**, 5117 (2006) [gr-qc/0604028].
- [20] P. Brax and C. van de Bruck, Class. Quant. Grav. **20**, R201 (2003) [hep-th/0303095]. L. A. Gergely, Phys. Rev. D **74**, 024002 (2006) [hep-th/0603244]. M. Demetrian, Gen. Rel. Grav. **38**, 953 (2006) [gr-qc/0506028].
- [21] D. Lovelock, J. Math. Phys. **12**, 498 (1971). D. Lovelock, J. Math. Phys. **13**, 874 (1972). S. H. Hendi and M. H. Dehghani, Phys. Lett. B **666**, 116 (2008) [arXiv:0802.1813 [hep-th]]. M. H. Dehghani and R. Pourhasan, Phys. Rev. D **79**, 064015 (2009) [arXiv:0903.4260 [gr-qc]]. S. H. Hendi, S. Panahyan and H. Mohammadpour, Eur. Phys. J. C **72**, 2184 (2012) [arXiv:1501.05841 [gr-qc]]. A. Sheykhi, H. Moradpour and N. Riazi, Gen. Rel. Grav. **45**, 1033 (2013) [arXiv:1109.3631 [physics.gen-ph]].
- [22] H. A. Buchdahl, Mon. Not. Roy. Astron. Soc. **150**, 1 (1970).
- [23] A. A. Starobinsky, Phys. Lett. B **91**, 99 (1980).
- [24] K. Bamba and S. D. Odintsov, JCAP **0804**, 024 (2008) [arXiv:0801.0954 [astro-ph]].
- [25] M. Akbar and R. G. Cai, Phys. Lett. B **648**, 243 (2007) [gr-qc/0612089]. K. Bamba and S. D. Odintsov, JCAP **0804**, 024 (2008) [arXiv:0801.0954 [astro-ph]]. G. Cognola, E. Elizalde, S. Nojiri, S. D. Odintsov, L. Sebastiani and S. Zerbini, Phys. Rev. D **77**,

- 046009 (2008) [arXiv:0712.4017 [hep-th]]. C. Corda, Int. J. Mod. Phys. D **18**, 2275 (2009) [arXiv:0905.2502 [gr-qc]]. S. Capozziello, F. Darabi and D. Vernieri, Mod. Phys. Lett. A **25**, 3279 (2010) [arXiv:1009.2580 [gr-qc]]. S. H. Hendi and D. Momeni, Eur. Phys. J. C **71**, 1823 (2011) [arXiv:1201.0061 [gr-qc]]. S. Asgari and R. Saffari, Gen. Rel. Grav. **44**, 737 (2012) [arXiv:1104.5108 [gr-qc]]. S. H. Mazharimousavi, M. Halilsoy and T. Tahamtan, Eur. Phys. J. C **72**, 1958 (2012) [arXiv:1109.3655 [gr-qc]]. S. G. Ghosh, S. D. Maharaj and U. Papnoi, Eur. Phys. J. C **73**, no. 6, 2473 (2013) [arXiv:1208.3028 [gr-qc]]. S. H. Hendi, B. Eslam Panah and R. Saffari, Int. J. Mod. Phys. D **23** (2014) [arXiv:1408.5570 [hep-th]].
- [26] R. Saffari and S. Rahvar, Phys. Rev. D **77**, 104028 (2008) [arXiv:0708.1482 [astro-ph]].
- [27] S. Soroushfar, R. Saffari, J. Kunz and C. Lämmerzahl, Phys. Rev. D **92**, no. 4, 044010 (2015) [arXiv:1504.07854 [gr-qc]].
- [28] R. Tharanath, J. Suresh, N. Varghese and V. C. Kuriakose, Gen. Rel. Grav. **46**, 1743 (2014) [arXiv:1404.6789 [gr-qc]].
- [29] T. Moon, Y. S. Myung and E. J. Son, Gen. Rel. Grav **43**, 3079 (2011) [arXiv:1101.1153 [gr-qc]].
- [30] A. Larranaga, Pramana Journal of Physics **78**, 697 (2012) [arXiv:1108.6325 [gr-qc]].